

Bifurcations leading to stochasticity in a cyclotron-maser system

R. Pakter, G. Corso, T. S. Caetano, D. Dillenburg, and F. B. Rizzato
*Instituto de Física-Universidade Federal do Rio Grande do Sul, Caixa, Postal 15051,
91501-970 Porto Alegre, RS, Brazil*

(Received 6 May 1994; accepted 1 August 1994)

This paper is concerned with the orbital dynamics of electrons in a cyclotron maser [C. Chen, *Phys. Rev. A* **46**, 6654 (1992)] with modulated maser fields. Amplitude modulation is a natural result of wave-particle energy exchanges, and for typical system parameters, the nonlinear bifurcations of periodic orbits are investigated as the modulation level increases. Attention is focused on primary stable orbits exhibiting the same periodicity as the modulation for low modulational levels. This interest is related to the fact that the destruction of these orbits is generally associated with considerable spread of chaos over the phase space. It is found that two groups of such orbits do exist, each group located in a particular region of the phase space. As the modulation level grows, the overall behavior can be classified as a function of the modulation frequency. If this frequency is large there are two orbits in the group; one undergoes an infinite cascade of period doubling bifurcations and the other simply collapses with neighboring unstable orbits. If the frequency is small the number of orbits is larger; the collapsing orbit is still present and some of the others may fail to undergo the period doubling cascade. © 1994 American Institute of Physics.

I. INTRODUCTION

There has been a growing interest in the study of stochastic relativistic interactions involving magnetized electrons and electromagnetic waves.

This is so because relativistic particles are likely to absorb large quantities of electromagnetic energy when the wave-particle interaction is chaotic.

It is relatively easy to generate chaotic orbits for this type of system. Indeed, by considering a stationary and homogeneous background magnetic field, it is generally shown that there exists a critical wave amplitude above which most of the particle phase-space becomes chaotic.¹ One noticeable case, however, does not follow this general rule: when the wave is circularly polarized and propagates parallel to the magnetic field, the dynamics can be shown to be exactly integrable. This kind of configuration, known as the cyclotron resonance maser accelerator (CRMA), is presently recognized as of importance both for laboratory and astrophysical beam studies.²

It has been shown³ that if the initial particle energies in a CRMA are small enough, these particles are rapidly bunched (in gyrophase) and subsequently accelerated to very large energies. On the other hand, if the initial energies are not small enough, phase bunching is absent and the average acceleration is very small.⁴ Considering these facts, one could say that unless the beam is carefully set at small initial energies, the global accelerating process tends to be ineffective.

Given that regular acceleration may not be always dominant in a CRMA, an issue to be addressed would be the possibility of deterministic stochastic acceleration. This could be the governing accelerating mechanism when beam control is poor or even absent. Such is the case of astrophysical beams in pulsar magnetospheres, for instance, where we point out that the usual wave-particle model is identical to the one we shall make use of.⁵ The analysis is also relevant for laboratory schemes where the accelerating length is long enough such that the effect of long-range inhomogeneities

cannot be discarded.⁶ The problem with stochastic processes, as mentioned before, is that constant amplitude modes generate only regular trajectories. One should note, however, that amplitude modulations may easily develop in this kind of system because of various factors. Among these, at least three can be considered as of relevance: (i) Low-energy particles, even if in small number, interact with the wave and cause pump depletion, so that higher-energy particles will view the resulting wave as a modulated train.⁴ (ii) Electromagnetic waves are unstable and can frequently develop nonlinear amplitude self-modulations.⁵ (iii) Slow modulations on the wave can also be produced in laboratories by slowly varying control parameters in an experiment.⁶

It shall be shown that amplitude modulations, no matter their precise origin, may indeed be responsible for the development of bifurcations and stochasticization of periodic orbits in cyclotron-maser systems.

Attention is focused on primary resonances generating trajectories with the same period as the modulation when the modulational amplitudes are small. This is done because this kind of trajectories tends to be the most stable present in the system, a feature leading to the conclusion that the respective orbital destabilization may be connected with global spread of chaos throughout the phase space.⁷ It shall be seen that two groups of orbits with these kind of characteristics are present for typical system parameters, each group located around a particular point of the phase space. One orbit of each group is a fixed point of the unperturbed dynamics, and when a small modulation is turned on, it acquires the same periodicity of the modulation, i.e., the modulation removes the corresponding orbital degeneracy. The other orbits turn out to be legitimate periodic orbits. It shall be found convenient to classify the overall behavior as a function of the modulation frequency. When this frequency is comparable to the fixed point gyrofrequency of one group, this group is, in fact, constituted only by two orbits. The orbit initially presenting degeneracy ceases to exist as it collapses with a

neighboring unstable periodic orbit; the other undergoes an infinite cascade of period doubling bifurcations. When the frequency is relatively small, the group contains more than two trajectories. The collapsing orbit behaves similarly as in the previous case. However, before it vanishes, it goes temporarily unstable within a band of the modulation amplitudes. Some of the others fail to undergo the period doubling sequence, a feature inhibiting global spread of chaos.

It should be remarked that the appropriate resonance analysis involves the calculation of particle gyrofrequencies. These gyrofrequencies should be fully renormalized by the presence of the large-amplitude maser modes, and as shall be seen, the calculations are made accordingly.

The paper is organized as follows. In Sec. II, one introduces the model, analyzes the regular motion generated by constant amplitude modes, and calculates the renormalized gyrofrequencies; in Sec. III, one numerically investigates the sequence of bifurcations for orbits presenting the same periodicity as the modulation for small modulational levels; and in Sec. IV, the work is concluded.

II. THE MODEL AND ITS REGULAR DYNAMICS

One starts by introducing the Hamiltonian of a test particle submitted to the combined action of a constant guiding magnetic field B_0 and an intense electromagnetic mode. Both the guide field and the wave vector of the fluctuating field are assumed to be aligned with the z axis of the chosen reference frame. The vector potential of the wave, \mathbf{A} , is written as

$$\frac{e}{mc^2} \mathbf{A} \equiv -\sqrt{\rho(t)} [\cos(kz - \omega t) \hat{\mathbf{x}} - \sin(kz - \omega t) \hat{\mathbf{y}}], \quad (1)$$

where $\rho(t) = \rho_0 [1 + \epsilon \cos(\Omega_{\text{mod}} t)]$ ($\epsilon \ll 1$), with Ω_{mod} as the modulation frequency, is now dependent on time. The elec-

tron charge is denoted by e , m is its mass, c is the velocity of light, ω is the wave frequency, and $k = \omega/c$. The test particle Hamiltonian is adimensionally written as

$$\mathcal{H} = mc^2 \{1 + [P_x + \sqrt{\rho} \cos(kz - \omega t)]^2 + [P_y + x - \sqrt{\rho} \sin(kz - \omega t)]^2 + P_z^2\}^{1/2}, \quad (2)$$

which can be cast in the guiding-center resonant form

$$\mathcal{H} = -\hat{\omega} I + \sqrt{1 + 2I + (\hat{\omega} I)^2 + 2\sqrt{2\rho} I \cos \phi} + \rho, \quad (3)$$

if one: (i) defines $\omega_{\text{co}} \equiv eB_0/mc$ and $\hat{\omega} \equiv \omega/\omega_{\text{co}}$; (ii) normalizes $t \rightarrow \omega_{\text{co}} t$, $\mathbf{r} \rightarrow (\omega_{\text{co}}/c)\mathbf{r}$, $\mathbf{P} \rightarrow \mathbf{P}/mc$, $\mathcal{H} \rightarrow \mathcal{H}/mc^2$; (iii) introduces canonical guiding-center coordinates $P_x = \sqrt{2I} \cos \phi$ and $x + P_y = \sqrt{2I} \sin \phi$; (iv) performs the time removal canonical transformation $I \rightarrow I$, $\mathcal{H} \rightarrow \hat{\omega} I + \mathcal{H}$, $\phi + \hat{\omega}(z - t) \rightarrow \phi$, and (v) finally introduces the adimensional modulation frequency as $\Omega = \Omega_{\text{mod}}/\omega_{\text{co}}$ setting $P_z \rightarrow 0$.

One now looks at the dynamics when $\rho = \rho_0 = \text{const}$.

For this exactly integrable case, where the Hamiltonian is a conserved quantity, Eq. (3) becomes $\mathcal{H}_0 \equiv \mathcal{H}(I, \phi, \rho = \rho_0) = E$ and we can introduce an action variable J , according to

$$J = \frac{1}{2\pi} \oint I(E, \phi) d\phi. \quad (4)$$

Then, on inserting $I(E, \phi)$ from Eq. (3) into Eq. (4) and inverting the resulting expression, one obtains

$$\mathcal{H}_0(J) = a \cos\left(\frac{b}{3} + c\right) - \frac{d}{3}, \quad (5)$$

where

$$a = \frac{2\sqrt{3 + 3\rho_0^2 + 8J + \hat{\omega}^{-2} + 4J^2 \hat{\omega}^2}}{3},$$

$$b = \arccos\left(\frac{(2/\hat{\omega}^3) - (18/\hat{\omega}) + (9\rho_0/\hat{\omega}) - (30J/\hat{\omega}) - 18J\hat{\omega} - 18\rho_0 J\hat{\omega} - 48J^2\hat{\omega} - 16J^3\hat{\omega}^3}{2(3 + 3\rho_0 + 8J + \hat{\omega}^{-2} + 4J^2\hat{\omega}^2)^{3/2}}\right),$$

$$c = 0, \frac{2\pi}{3}, \frac{4\pi}{3},$$

and

$$d = 2J\hat{\omega} - \frac{1}{\hat{\omega}}.$$

Variable c takes three distinct values, but only the first and third ones have physical meaning. The second generates negative numerical values of \mathcal{H}_0 which can not correspond to any physically possible dynamical branch because the Hamiltonian is always positive, as can be seen if one writes Eq. (3) (for the most dangerous case $\cos \phi = -1$) in the equivalent form

$$(\mathcal{H}_0)_{\text{min}}$$

$$= -\hat{\omega} I + \sqrt{(\hat{\omega} I)^2 + 1 + I + 2\sqrt{2\rho_0} I + (2\sqrt{2\rho_0} - \sqrt{I})^2} > 0. \quad (6)$$

In what follows $\hat{\omega}$ shall be chosen $\hat{\omega} = 1/\sqrt{1 + \rho_0}$, which corresponds to the autoresonance regime.³ The physical solutions correspond to the two classes of orbits shown in Fig. 1. The value of ρ_0 is taken equal to one here and further on, since we are considering intense electromagnetic modes. Each class revolves around its own unperturbed central fixed point which shall be called CFP_{\pm} , with $\text{CFP}_+ = \text{CFP}(c=0)$ and $\text{CFP}_- = \text{CFP}(c=4\pi/3)$. The coordinates of CFP_{\pm} , (ϕ_{\pm}, I_{\pm}) , are such that $\cos \phi_{\pm} = \pm 1$ and $\partial_I \mathcal{H}_0(\phi_{\pm}, I_{\pm}) = 0$ and, as mentioned in Sec. I, these are fixed points of the unperturbed dynamics.

The renormalized gyrofrequencies for orbits around the fixed points, ω_{\pm} , are obtained as functions of J from ω_{\pm}

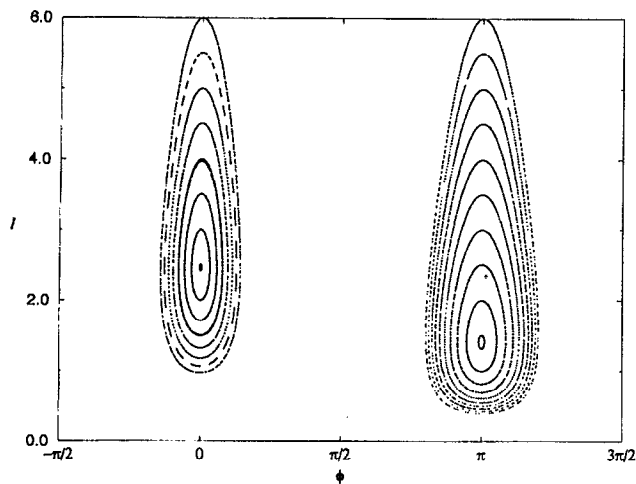


FIG. 1. A full portrayal of the unperturbed phase space ($\epsilon=0$, $\rho_0=1.0$).

$= \partial_J \mathcal{H}_0|_{\text{CFP}_\pm}$ and are plotted in Fig. 2 for the + and - branches. Similarly to the case where no wave is present, it is seen that the gyrofrequencies decrease with J . This means that primary resonances located at J_n ($n=\pm 1, \pm 2, \dots$) with

$$n\omega_\pm(J_n) = \Omega \quad (7)$$

and secondary resonances located at $J_{n,p}$ with

$$n\omega_\pm(J_{n,p}) = p\Omega, \quad (8)$$

and $p \neq \pm 1$, are such that larger n 's correspond to larger $J_{n,p}$'s.

To illustrate the typical bifurcational behavior of the system, the following analysis is performed for initial conditions within the rightmost lobule (the “-” lobule) of Fig. 1. The choice is dictated by the fact that this is the lobule first developing substantial degrees of chaoticity.

In order to be consistent with existing results the following condition indicated in previous wave-particle numerical simulations is assumed:⁴ $\omega_-(J=0) > \Omega$. This, in turn, implies that the lower primary resonance present in the system will be the one with $n = +1$.

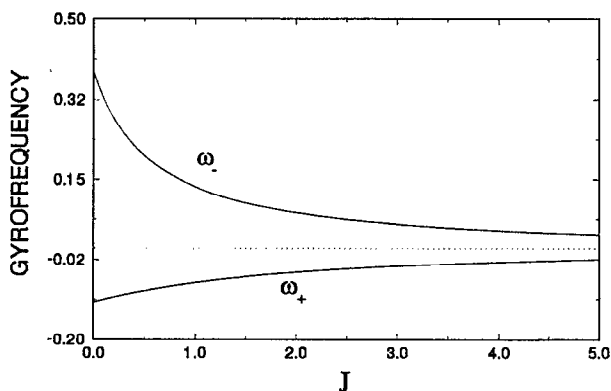


FIG. 2. The frequencies ω_+ and ω_- as a function of the action J .

We finally mention that in a periodic Poincaré plot a $J_{n,p}$ resonance appears as a resonant pendulum-like island chain with its respective elliptic and hyperbolic fixed points. These fixed points are in fact a discrete-mapping version of periodic orbits and whenever mentioned in the text they should be understood within this context. Elliptic points of a $J_{n,p}$ resonance shall be denoted as $(J_{n,p})_e$ and hyperbolic points as $(J_{n,p})_h$.

III. NUMERICAL INTEGRATION OF THE EQUATIONS OF MOTION

All the simulations shall be performed on basis of stability analysis and Poincaré plots. These two approaches should complement each other.

A. Stability analysis

The behavior of the fixed points as a function of the modulation amplitude ϵ may be accurately followed with help of a Newton-Raphson algorithm^{8,9} and the respective stability diagrams. In the stability diagrams, one plots the so-called stability index (α) of a particular periodic orbit as a function of the perturbing parameter, the factor ϵ in our case. If $|\alpha| < 1$ the corresponding orbit is stable (elliptic fixed points) and if $|\alpha| > 1$ the orbit is unstable (hyperbolic fixed points). Two kinds of orbital bifurcations are usual for this kind of Hamiltonian system. In a forward or backward period doubling bifurcation, periodic orbits undergo direct or inverse period doubling bifurcation with $\alpha = -1$ at the bifurcation point. In a backward tangent bifurcation, existing elliptic points of a periodic orbit collapse with hyperbolic points of a neighboring orbit of the same periodicity;⁹ in this case, both orbits simply cease to exist with $\alpha = +1$ at the end point.

These are the basic characteristics that shall be needed to clarify the stability properties of the orbits.

The analysis is performed for the two representative regimes of frequency modulation introduced before. One first considers the case of relatively large frequencies implying small wave-particle mismatches for which a conveniently defined scaled mismatch $\hat{\delta}_-$ satisfies

$$\hat{\delta}_- \equiv \left| \frac{\omega_- - \Omega}{\omega_-} \right| \ll 1. \quad (9)$$

To accomplish that one takes $\Omega=0.32$, which implies $\hat{\delta}_- \sim 0.16$. This is the case portrayed in the sequence represented in Fig. 3.

Two points with the same modulational periodicity appear in the figure. One of them is the CFP₋ and the other is the elliptic point of the J_1 resonance, $(J_1)_e$. The figure shows that the CFP₋ vanishes when it collapses with $(J_1)_h$, and that later on $(J_1)_e$ undergoes period doubling bifurcation. We have accompanied two of such bifurcations, and a search for higher-order stable bifurcated points at $\epsilon=1.0$ failed to indicate the presence of this kind of orbits. The conclusion is that $(J_1)_e$ undergoes an infinite cascade of bifurcations as the modulational level grows to the maximum allowed value. In this situation, one should expect a reasonable degree of stochasticity over the phase space.

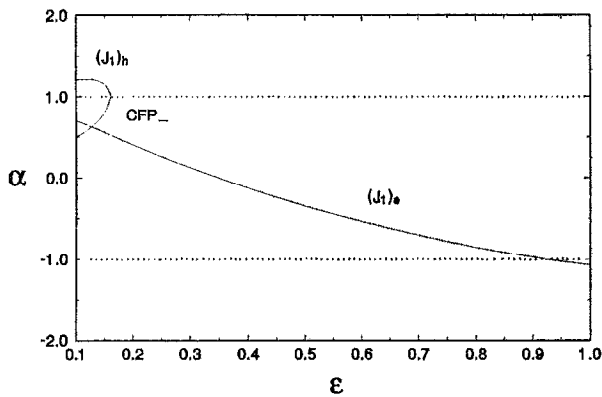


FIG. 3. The stability index α in the small mismatch case, $\Omega=0.32 \Rightarrow \hat{\delta} \sim 0.16$.

The other limiting case, the case of large values of $\hat{\delta}$, is represented in Fig. 4 where one takes $\Omega=0.1$ with $\hat{\delta} \sim 0.75$. One sees that the overall orbital behavior turns out to be different from the previous case.

To start with the analysis, one can note that in this case, not only a resonance of the type J_1 is present as before. Resonances of the type $J_{1,2}$ and $J_{1,3}$ ($J_1 > J_{1,2} > J_{1,3}$) may also be found due to the fact that Eq. (8) can now be solved not only for positive values of J_1 , but for positive values $J_{1,2}$ and $J_{1,3}$ as well.

From the figure one sees that the CFP_- still vanishes via a backward tangent bifurcation as it collapses with a neighboring hyperbolic point. One should note, however, that this hyperbolic point is no longer the hyperbolic point of the J_1 primary resonance; now it is $(J_{1,3})_h$, the closest hyperbolic point to the CFP_- with periodicity $n=1$.

Next, one can observe that CFP_- passes through an unstable region before it regains stability and collapses. In this unstable region denoted by "u" in the figure, the CFP_- undergoes one single period doubling bifurcation. To prevent the appearance of the "u" region, the hyperbolic point should be located at very close proximity to the CFP_- , which indicates that such a kind of temporary unstable behavior may be typical in the large mismatch case. In the small mismatch case, the larger sizes of the resonant island

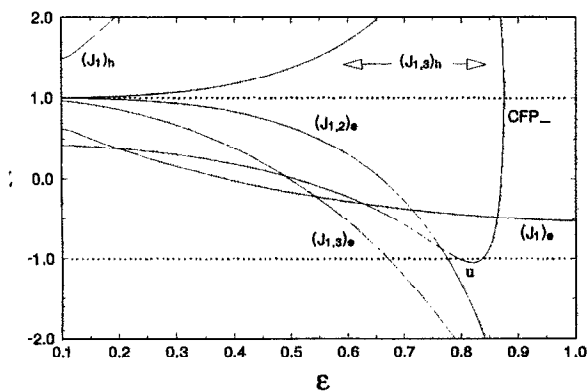


FIG. 4. Stability index in the large mismatch case, $\Omega=0.1 \Rightarrow \hat{\delta} \sim 0.75$.

seems to cause the collapse without the preceding destabilization of the CFP_- . This unstable feature shall be also appreciated with help of the appropriate Poincaré plot.

Finally, one considers the behavior of the elliptic points $(J_1)_e$, $(J_{1,2})_e$, $(J_{1,3})_e$. Among these points one observes that only the first, $(J_1)_e$, is not destabilized for ϵ below its maximum allowed value. The other two undergo full cascades of period doubling sequences. As in the previous situation, one could not find any higher-order stable orbits originating from any of them, and the conclusion is that both elliptic points undergo full period doubling cascades. In spite of the period doubling sequences, the lingering presence of $(J_1)_e$ leads to the conclusion that global spread of chaos should be somewhat inhibited.

Let us now turn to Poincaré plots to examine some of the peculiar features revealed by the diagrams.

B. Poincaré plots

In Fig. 5, a sequence of plots of the $\Omega=0.32$ case is presented for an increasing modulation amplitude. In Fig. 5(a), one observes both the CFP_- and the full J_1 resonance, with both hyperbolic and elliptic points present. In Fig. 5(b), only the elliptic point $(J_1)_e$ survives, and in Fig. 5(c), ϵ is just above the period doubling amplitude observable in Fig. (3). Also the case $\epsilon=1.0$ has been considered; a search for higher-order stable fixed points originated from $(J_1)_e$ [we have launched several grids of 50×50 initial conditions close to last position of $(J_1)_e$], as mentioned before, failed to detect any. The conclusion is that $(J_1)_e$ probably follows the full cascade of bifurcations to chaos as one proceeds from small to the largest possible modulational amplitude. One, therefore, associates small mismatches with a tendency to infinite period doubling cascades for $(J_1)_e$.

In Fig. 6, the $\Omega=0.1$ case is examined. In Fig. 6(a), one can observe the CFP_- along with the full J_1 and $J_{1,2}$ and $J_{1,3}$ resonances. Note that the locations of the fixed points on the $\phi \times I$ plane satisfy $(I_{1,(1,3)})_h > (I_{1,(1,3)})_e$ and $(I_{1,2})_h < (I_{1,2})_e$. In Fig. 6(b), one magnifies the CFP_- region in its unstable period doubled region to show the period doubled regime. In Fig. 6(c), the restabilized CFP_- is shown. Finally, in Fig. 6(d), the presence of $(J_1)_e$ is confirmed for the largest perturbing value of ϵ , $\epsilon=1.0$. Global chaos is therefore inhibited, because orbits with initial condition close enough to $(J_1)_e$ can never be stochastically accelerated.

IV. FINAL REMARKS

To summarize, the transition from regular to global chaotic dynamics has been analyzed in a system of particles subjected to the combined action of strong guiding magnetic fields and modulated high intensity electromagnetic modes. For typical system parameters of a cyclotron-maser accelerator, we have analyzed classes of stable orbits with the same periodicity as the modulations when the modulational levels are low. Two were identified as being of foremost importance. One of them was referred to as the central fixed point orbit, CFP_- , and the other as the periodic orbits $(J_{1,p})_e$. Depending on the mismatch between particle renormalized gyrofrequency and wave frequency, different routes to global

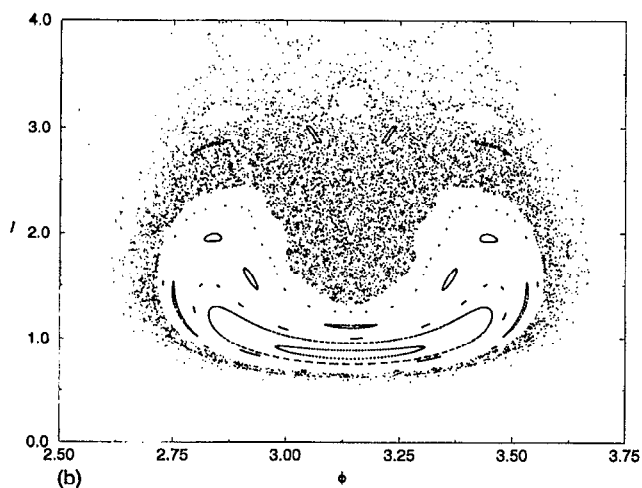
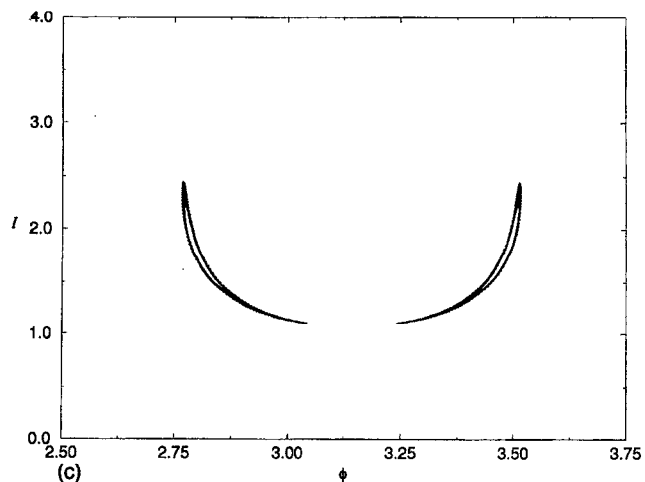
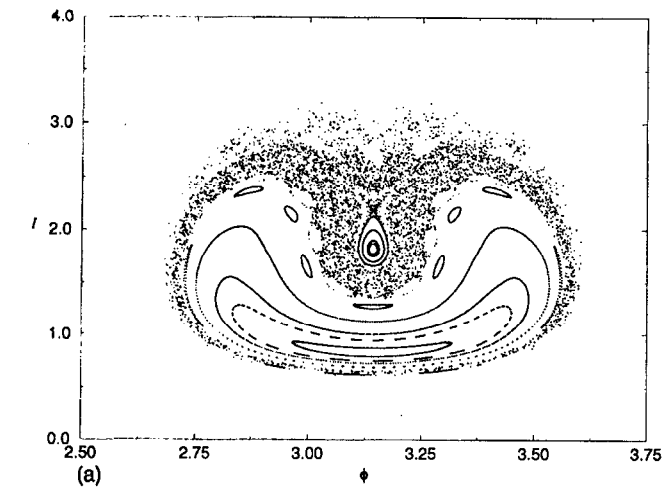


FIG. 5. Bifurcation sequence in the small mismatch case, $\hat{\delta} \sim 0.16$. We take $\epsilon(a, b, c) = 0.14, 0.16$, and 0.937 , respectively.

spread of stochastic trajectories may take place. Among other results, it was found out that for small scaled mismatches the CFP₋ is destroyed and that only a $(J_1)_e$ which undergoes a complete sequence of period doubling bifurcations does exist. For large mismatches the CFP₋ still vanishes but $(J_1)_e$ fails to undergo the period doubling cascade. In this case, however, other orbits with $p=1$ and $p=2$ which do undergo the period doubling cascade are present. For even larger mismatches, one expects to see the birth of $J_{1,p}$ with larger values of p , with the ones with relatively small p values failing to bifurcate. In the general case of large mismatches, global spread of chaos is therefore inhibited. These results are expected to be of relevance in the description of maser accelerating processes whenever the maser beams are likely to be slowly modulated. This could be the case of laboratory systems where the maser beams are externally modulated by varying control parameters (like the waveguide radius, for instance)⁶ or the case of astrophysical particle jets where the radiation beam is both self-modulated⁵ or modulated by wave-particle energy exchange effects.^{3,4} In the magnetosphere of pulsars where $e|A|_{\text{maser}}/mc^2 \sim \rho_0 \sim 1.0$, for instance, the modulational frequencies can be easily found in the range

$\Omega_{\text{dimensional}}/\omega_{\text{maser}} \sim \Omega \sim 0.01 > \omega_-$ or larger, which effectively may set the system in the large mismatch regime.

As far as small mismatches are concerned, we point out that the high intensity regime $\rho_0 \sim 1$ is characterized by modulational frequencies that can be of the same order of magnitude as the linear frequencies of the electromagnetic carrier modes, where we recall that for $\rho_0 = 1$ one has $\Omega/\omega_- \sim 0.46$. Rigorously speaking, one could not refer to this fast process as a modulational one, because it would not be possible to precisely define the slowly varying amplitude of the carrier and the corresponding well-defined high frequency. It is to be understood that we have used this terminology throughout the text for sake of simplicity.

In any case, these "fast modulations" can indeed arise in systems with a single spatial mode (space periodicity determined by a single wave vector k) as the one we are considering. In fact, it can be seen that the modulational time scale in a self-consistent model linearly depends on the particle density.³ In low-density beams with 10^8 electrons/cm³, for instance, the modulation frequency is much smaller than the carrier frequency. For larger densities such as 10^{10} electrons/cm³, on the other hand, the frequencies become

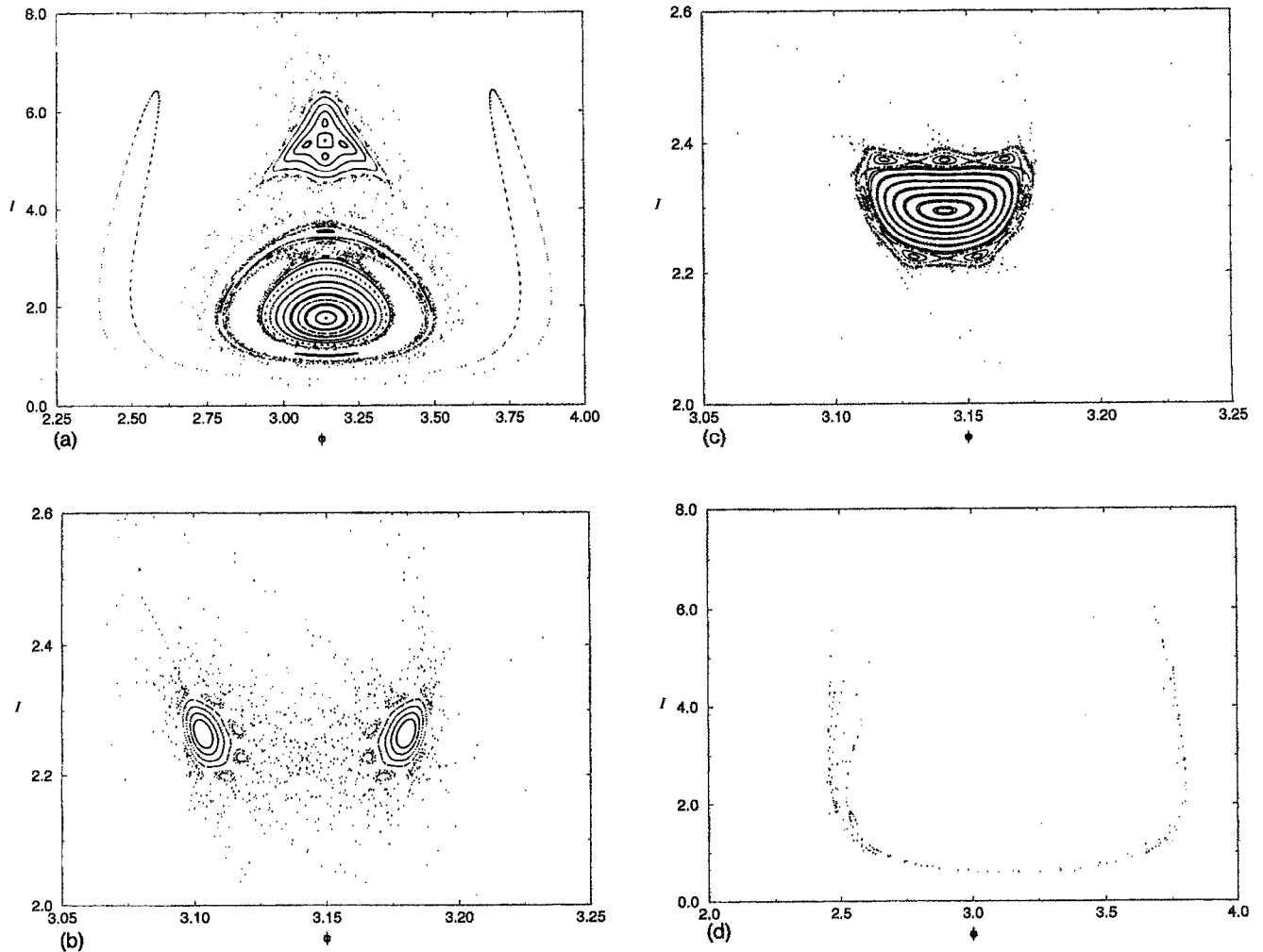


FIG. 6. Bifurcation sequence in the large mismatch case, $\delta \sim 0.75$. We take $\epsilon(a, b, c, d) = 0.5, 0.82, 0.84$, and 1.0 , respectively.

comparable and the slow modulation assumptions must be abandoned.

If alternatively one looks at the problem without considering any self-consistent effects, fast modulations could be seen as driven by the beating of a pair of waves with not so close carrier frequencies ω_1 and ω_2 . Indeed, one would have a beat electromagnetic field characterized by two frequencies $1/2(\omega_1 + \omega_2) \equiv \Omega_+$ (the average carrier frequency) and $1/2(\omega_1 - \omega_2) \equiv \Omega_-$ (the “modulation” frequency), whose ratio could be arbitrary, depending on the choice of ω_1 and ω_2 . This could be the model describing self-modulations of ultraintense electromagnetic modes propagating in plasmas—in this kind of system it is known that the modulational time scale reduces with increasing wave amplitude.⁵ Note that in this situation each wave would contribute its own wave vector to the process. While our model employs only one single spatial mode and therefore can not entirely reflect this spatiotemporal beat configuration, there is no reason to expect that the general conclusions on the bifurcation behavior as a function of the mismatch δ (now redefined appropriately in terms of Ω_+ and Ω_-) would suffer any considerable changes.

ACKNOWLEDGMENTS

Useful discussions with Professor Abraham C.-L. Chian are acknowledged. Useful comments and suggestions by an anonymous referee are also acknowledged.

This work was partially supported by Financiadora de Estudos e Projetos (FINEP), Conselho Nacional de Desenvolvimento Científico (CNPq), and Pró-Reitoria de Pesquisa e Graduação (PROPESP-UFRGS), Brazil and numerical computing was partially performed on the CRAY YMP-2E at the Universidade Federal do Rio Grande do Sul Supercomputing Center.

¹K. Akimoto and H. Karimabadi, *Phys. Fluids* **31**, 1505 (1988).

²C. Chen, *Phys. Rev. A* **46**, 6654 (1992).

³R. Pakter, R. S. Schneider, and F. B. Rizzato, *Phys. Rev. E* **47**, 3787 (1993); **49**, 1594 (1994).

⁴R. Pakter and F. B. Rizzato, *Phys. Scr.* **48**, 598 (1993).

⁵A. C.-L. Chian and C. F. Kennel, *Astrophys. Space Sci.* **97**, 9 (1983).

⁶L. Friedland, *Phys. Plasmas* **1**, 421 (1994).

⁷W. Rozmus and P. P. Goldstein, *Phys. Rev. A* **38**, 5745 (1988).

⁸G. Polymilis and K. Hyzanidis, *Phys. Rev. E* **47**, 4381 (1993).

⁹G. Corso and F. B. Rizzato, “Hamiltonian bifurcations leading to chaos in a low-energy relativistic wave-particle system,” to appear in *Physica D*.